AIAA JOURNAL
Vol. 33, No. 1, January 1995

Technical Notes

TECHNICAL NOTES are short manuscripts describing new developments or important results of a preliminary nature. These Notes cannot exceed 6 manuscript pages and 3 figures; a page of text may be substituted for a figure and vice versa. After informal review by the editors, they may be published within a few months of the date of receipt. Style requirements are the same as for regular contributions (see inside back cover).

Viscous-Inviscid Interaction Method for Unsteady Low-Speed Airfoil Flows

Ismail H. Tuncer,* John A. Ekaterinaris,† and Max F. Platzer‡
Naval Postgraduate School, Monterey, California 93943

Introduction

THE computational efficiency in computing the viscous flowfields around airfoils may be improved by splitting the flow domain into an inviscid potential flow zone and a viscous boundary-layer/separated flow zone and by solving the distinct governing equations in each zone. In conventional viscous/inviscid interaction methods[1] this is achieved by solving the boundary-layer equations around the airfoil and assuming potential flow for the outer flowfield. This approach has the well-known limitations of the boundary-layer equations. In addition, it needs an unsteady wake modeling in the computations of unsteady flowfields. These complications suggest the desirability of exploring a Navier-Stokes based viscous-inviscid interaction approach for the computation of unsteady flowfields.

We have coupled a Reynolds-averaged Navier-Stokes solver with a potential flow panel code in an attempt to split the flowfield into viscous and inviscid flow zones with the objective to reduce the computational domain in which Navier-Stokes equations are solved. In the present work, we are mainly interested in unsteady flows. Summa et al.[2] originally applied a similar concept of coupling potential and viscous flow solution methods to steady flows. In comparison to the full Navier-Stokes solvers in which the computational domain is required to extend approximately 15 chord lengths from the airfoil surface, in this methodology the computational domain boundaries can be placed as close as one-fifth of a chord length from the airfoil surface. The reduced computational domain encompasses the viscous boundary layer/wake regions in the close proximity of the airfoil, and the adjacent inviscid flow zone between the viscous flow zone and the outer boundary of the computational domain. The boundary conditions at the outer boundary are obtained from the potential flow solution. The boundary conditions for the potential flow solution are, in turn, computed by the Navier-Stokes solver on the inviscid flow zone beyond the boundary layers. Thus, the potential and Navier-Stokes flow solutions are coupled through their boundary conditions. The vortical wake in the unsteady flows is modeled with concentrated wake vortices. This inviscid wake modeling fully captures the unsteadiness contained in the wake.

Received Feb. 9, 1994; revision received July 19, 1994; accepted for publication July 28, 1994.This paper is declared a work of the U.S. Government and is not subject to copyright protection in the United States.

*Research Associate, Department of Aeronautics and Astronautics. Member AIAA.

†Research Associate Professor, Department of Aeronautics and Astronautics. Senior Member AIAA.

‡Professor, Department of Aeronautics and Astronautics. Associate Fellow AIAA.

Navier-Stokes/Potential Flow Interactive Solution Method

In the Navier-Stokes/potential flow interactive solution method (NSPOT), the computational domain is partitioned into two zones, a near-field and a far-field zone. Figure 1 shows the near-field zone around an airfoil and its wake on a C grid. The solid line in the figure encloses the outer boundary of the near-field zone S_o. The near-field zone encompasses the viscous boundary-layer and wake regions and the inviscid flow region between the outer boundary S_o and the viscous flow regions. The Navier-Stokes (NS) equations are solved in the entire near-field zone. An inner boundary S_i which is denoted by a dashed line in Fig. 1, is placed in the inviscid flow region of the near-field computational domain. The source and vortex panels used in the solution of the potential flow equation are placed on S_i. The region outside of S_o, which extends to the freestream flow conditions in all directions, is the far-field zone. The flowfield in the far-field zone is assumed to be inviscid and irrotational and, thus, may be computed by a Potential flow solution.

In the computation of unsteady flowfields, the downstream edge of the inner boundary S_{iw} is placed in the close vicinity of the airfoil as shown in Fig. 1. It cuts through the wake at 10–50% chord length from the airfoil trailing edge. For unsteady flows, it was found to be necessary to model the vortex shedding at the intersection of S_{iw} and the viscous wake. Whereas, in the computation of steady flowfields the S_{iw} is extended beyond the computational grid. The extended S_i boundary encloses all of the vorticity in the wake, and no vortex shedding is required.[3]

Potential Flow Solver

The flowfield beyond the inner boundary S_i is assumed to be inviscid, irrotational, and isentropic. The governing equations in terms of the disturbance potential read

$$\frac{\partial \rho}{\partial t} + \nabla \cdot (\rho \nabla \phi) = 0 \tag{1}$$

$$\frac{\partial}{\partial t}(\nabla \phi) + \nabla\left(\frac{V^2}{2}\right) + \frac{\nabla p}{\rho} = 0 \tag{2}$$

For low Mach number flows, density variations in Eq. (1) are first dropped, and the resulting Laplace's equation $\nabla^2 \phi = 0$ is solved with a panel method using source/sink and vorticity singularity solutions to satisfy the appropriate boundary conditions on S_i. The velocities computed by the panel method on S_o are then corrected for compressibility effect using the Laitone compressibility correction.[3] The pressure and density fields on S_o are evaluated by using the isentropic relation between p and ρ and then, by integrating Eq. (2) for pressure[4]

$$p = p_\infty \left[1 + \frac{(\gamma - 1)}{\gamma} \frac{\rho_\infty}{p_\infty}\left(\frac{V_\infty^2 - V^2}{2} - \frac{\partial \phi}{\partial t}\right)\right]^{\frac{\gamma}{\gamma - 1}} \tag{3}$$

where V^2 is computed with the compressibility corrected velocities.

In unsteady flows, as the solution is marched in time, a discrete vortex is shed from the S_{iw} boundary. The magnitude of the shed vortex is based on the time rate of change of circulation on the S_i boundary: $\gamma_w^n = -(\Gamma^n - \Gamma^{n-1})$, where superscript n denotes the time step. The circulation Γ is computed from the integration of the tangential velocity on S_i given by the NS solution. Once the vortices are shed, they are convected downstream. The convection

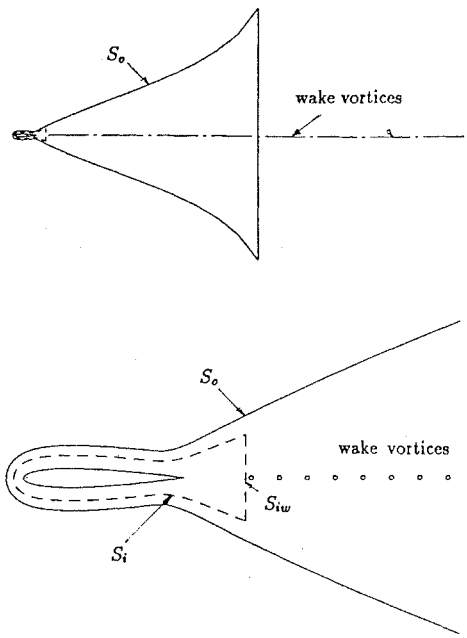

Fig. 1 Computational domain for the Navier-Stokes/potential flow interactive solution method.

velocity is approximated by an empirical formula[4] which states that the depression in the velocity profile decreases as $1/\sqrt{x}$.

Navier-Stokes Solver

The strong conservation-law form of the two-dimensional, thin-layer Navier-Stokes equations in a curvilinear coordinate system (ξ, ζ) along the axial and normal direction respectively, is given as follows:

$$\partial_t \hat{Q} + \partial_\xi \hat{F} + \partial_\zeta \hat{G} = Re^{-1}\partial_\zeta \hat{S} \tag{4}$$

where $\hat{Q}$ is the vector of conservative variables, $\hat{F}$ and $\hat{G}$ are the inviscid flux vectors, and $\hat{S}$ is the thin-layer approximation of the viscous fluxes in the ζ direction normal to the airfoil surface.[5] The flowfield is assumed to be fully turbulent, and the Baldwin-Lomax turbulence model is used to evaluate the eddy viscosity.

The numerical integration is performed using an upwind biased, factorized, iterative, implicit, numerical scheme[5] given by

$$\begin{aligned}&\left[I + h_\xi\left(\nabla_\xi^b \tilde{A}_{i,k}^+ + \Delta_\xi^f \tilde{A}_{i,k}^-\right)\right]^p \\ &\times \left[I + h_\zeta\left(\nabla_\zeta^b \tilde{B}_{i,k}^+ + \Delta_\zeta^f \tilde{B}_{i,k}^- - Re^{-1}\delta_\zeta \tilde{M}_{i,k}\right)\right]^p \left(\tilde{Q}_{i,k}^{p+1} - \tilde{Q}_{i,k}^p\right) \\ &= -\Big[\left(\tilde{Q}_{i,k}^p - Q_{i,k}^n\right) + h_\xi\left(\hat{F}^p_{i+\frac{1}{2},k} - \hat{F}^p_{i-\frac{1}{2},k}\right) \\ &+ h_\zeta\left(\hat{G}^p_{i,k+\frac{1}{2}} - \hat{G}^p_{i,k-\frac{1}{2}}\right) - Re^{-1}h_\zeta\left(\hat{S}^p_{i,k+\frac{1}{2}} - \hat{S}^p_{i,k-\frac{1}{2}}\right)\Big]\end{aligned} \tag{5}$$

In Eq. (5), the superscript n denotes the time step and p refers to Newton subiterations within each time step. The inviscid fluxes $\hat{F}$ and $\hat{G}$ are evaluated using Osher's third-order-accurate upwinding scheme. The flux Jacobian matrices $\tilde{A}^\pm$ and $\tilde{B}^\pm$ are evaluated by the Steger-Warming flux-vector splitting.

Results and Discussion

We investigated unsteady flowfields around a NACA 0012 airfoil undergoing pitching motions and steady flowfields around stationary airfoils held at various incidences. A 181×81 point C-type baseline grid with 120 points around the airfoil and 81 points in the normal direction was employed. The normal spacing at the airfoil surface was 0.00005. The computational grid for NSPOT computations was obtained from the baseline grid by excluding the grid lines beyond the specified S_o boundary in the transverse direction. The inner boundary S_i was located 4–6 grid points inside S_o.

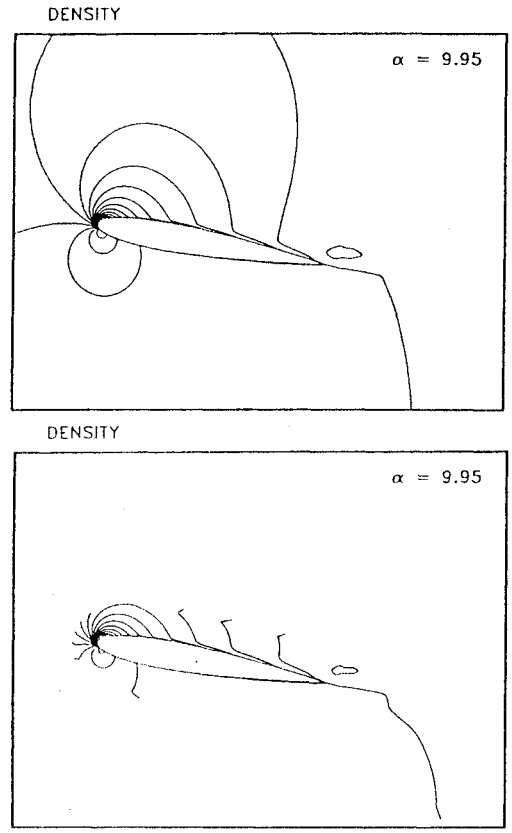

Fig. 2 Flowfield computed by NS and NSPOT, $S_o = 0.15c$, sinusoidally oscillating airfoil, $\alpha = 5 + 5\cos(\omega t)$, $\omega c/2U_\infty = 0.099$, $M_\infty = 0.3$, and $Re = 3.93 \times 10^6$.

Flow over an Oscillating Airfoil

We first studied the unsteady flowfield around a NACA 0012 airfoil undergoing an oscillatory motion with a reduced frequency, $k = \omega c/2U_\infty = 0.099$ and $\alpha(t) = 5 + 5\cos(\omega t)$. Here ω is the frequency of the oscillatory motion, and α is in degrees. The pitching axis was located at $0.25c$. The flowfield was computed at $M_\infty = 0.3$ and $Re = 3.93 \times 10^6$. In the NSPOT computations, the computational boundaries were located at $S_o = 0.15c$ and $S_{iw} = 0.30c$. This outer boundary location sets the computational grid size to 181×49, which gives about 40% savings in the total number of grid points.

Figure 2 shows the flowfields computed by NSPOT and NS solutions in terms of density contours with the same contour values. The quantitative agreement in the density contours shows that the NSPOT solution captures the compressibility of the flowfield accurately. It may be concluded that for low Mach number flows, the density variations in the continuity equation Eq. (1) may be omitted when this equation is solved on S_i, provided that the computed velocities on S_o are corrected for compressibility effects, and the evaluation of pressure includes the compressibility effects through isentropic flow relations. Figure 3 shows the boundary-layer profiles at the maximum angle of attack, $\alpha = 10$ deg ↑. The + marks on the profiles correspond to every fifth grid point. The predictions of the NSPOT and NS solutions agree quite well.

Figure 4 shows the unsteady aerodynamic load hysteresis loops computed by NS and NSPOT solutions and the measurements of McAlister et al.[6] The NS and NSPOT predictions, in general, agree well except for a slight deviation in the drag and moment coefficients as the angle of attack increases. This is mainly caused by the slight underprediction of the stagnation pressure in the NSPOT computation, which may be attributed to the compressibility effect. As the oscillatory motion advances into the second cycle, the lift predicted by NSPOT is slightly higher than the NS prediction and is not exactly periodic. This behavior is attributable to the differences in the vortical wake computations. In the NS computations, the downstream boundary extends 10 chord lengths, and the vorticity in the wake leaves the computational domain when it reaches the down-

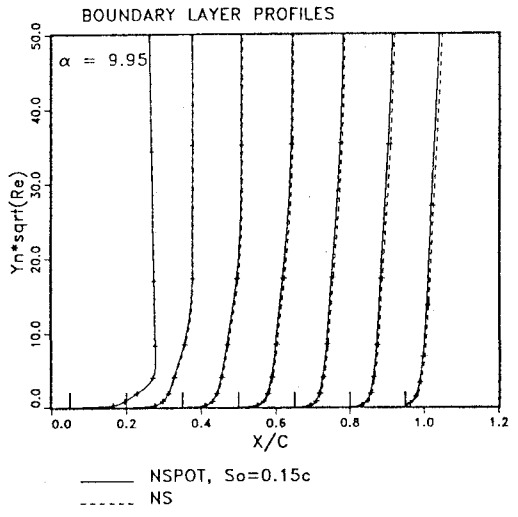

Fig. 3 Boundary-layer profiles, sinusoidally oscillating airfoil, $\alpha = 5 + 5\cos(\omega t)$, $\omega c/2U_\infty = 0.099$, $M_\infty = 0.3$, and $Re = 3.93 \times 10^6$.

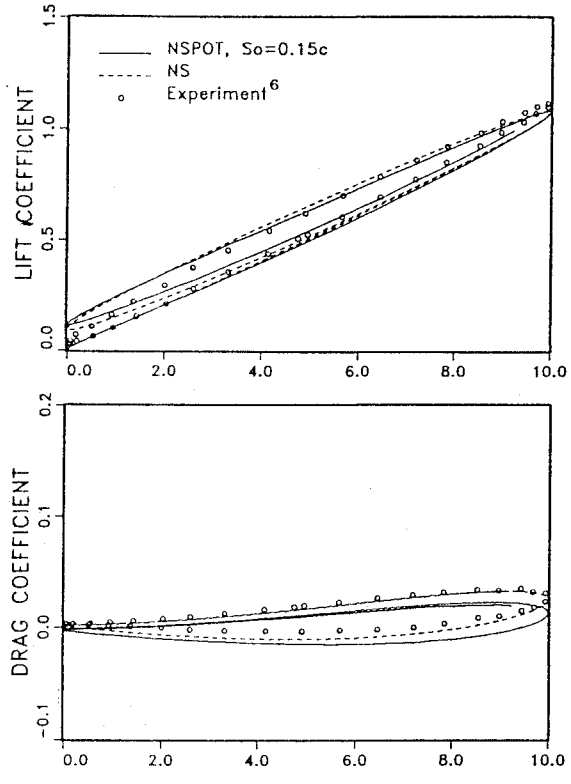

Fig. 4 Time history of the unsteady aerodynamic loads, sinusoidally oscillating airfoil, $\alpha = 5 + 5\cos(\omega t)$, $\omega c/2U_\infty = 0.099$, $M_\infty = 0.3$, and $Re = 3.93 \times 10^6$.

stream boundary. However, in NSPOT, all of the shed vortices are conserved and are accounted for.

The accuracy of the computed aerodynamic loads deteriorates when the outer boundary S_o is located as close as $0.10c$ from the airfoil, for which S_i happens to be located at $0.05c$ from the airfoil.[4] In this case, the S_i boundary is placed so close that it does not completely enclose the vortical field around the airfoil. Similarly, NSPOT computations were found to be insensitive to the location of the S_{iw} in the $0.10c-0.60c$ range. However, the accuracy of the computations degraded when S_{iw} is placed beyond one chord length from the trailing edge.[4] This behavior is attributed to the weakened coupling between shed vortices and the unsteady wake. The longer the unsteady viscous wake ahead of the vortex shedding boundary S_{iw}, the more the unsteady effects are delayed and suppressed.

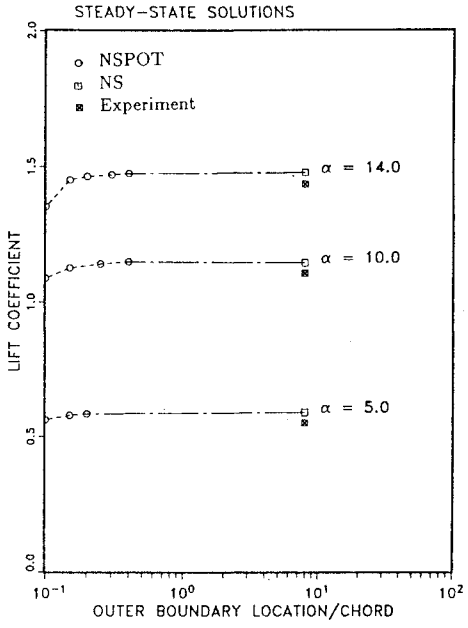

Fig. 5 Steady-state lift values computed by NS and NSPOT.

Steady Flows

We computed steady flowfields around a NACA 0012 airfoil at $M_\infty = 0.30$, $Re = 3 \times 10^6$ and $\alpha = 5$, 10, and 14 deg. NSPOT computations produced a 47%–30% grid point savings over the full NS computations when the S_o location was varied between $0.10c$ and $0.40c$. Figure 5 shows the lift values computed by NS and NSPOT solutions as a function of S_o location and incidence. It is clearly seen that the Navier-Stokes/potential flow interactive solution method is highly accurate and stable. At low incidences, such as $\alpha = 5$ deg, for which the boundary-layer thickness is relatively thin, the outer boundary S_o can be placed at a distance as close as $0.10c$ distance from the airfoil surface. As the vortical flow region grows at higher incidences, the S_o location has to be placed farther away. However, for mostly attached flows up to $\alpha = 14$ deg, the accuracy of the computed lift value with S_o located at $0.20c$ does not degrade more than 1%. At incidences higher than $\alpha = 14$ deg, the NS solution predicted massive flow separation. For massively separated flows, NSPOT computations cease to be efficient, since the outer boundary S_o has to be placed more than two chord lengths away from the airfoil as the extent of the vortical region grows.

Concluding Remarks

We have developed a Navier-Stokes/potential flow interactive solution method for unsteady and steady flows. This method confines the Navier-Stokes computations to the close proximity of the vortical boundary-layer and the wake regions. The method is capable of predicting low Mach number, attached or mildly separated flowfields as accurately as the full domain Navier-Stokes solutions. For a typical flowfield, the Navier-Stokes/potential flow interactive solution method is about 40% more efficient than the full Navier-Stokes method in terms of CPU times.

Acknowledgments

This investigation was supported by the Naval Air Warfare Center, Weapons Division, China Lake, California and by the National Research Council Research Associateship Program.

References

[1]Cebeci, T., Platzer, M. F., Jang, H. M., and Chen, H. H., "An Inviscid-Viscous Interaction Approach to the Calculation of Dynamic Stall Initiation on Airfoils," *Journal of Turbomachinery*, Vol. 115, No. 4, 1993, pp. 714–723.

[2]Summa, J., Strash, D., and Yoo, S., "Zonal Flow Analysis Method for Two-Dimensional Airfoils," *AIAA Journal*, Vol. 30, No. 2, 1992, pp. 548–549.

[3]Tuncer, I. H., Ekaterinaris, J. A., and Platzer, M. F., "A Viscous-Inviscid Interaction Method for 2-D Unsteady, Compressible Flows," AIAA Paper 93-3019, June 1993.
[4]Tuncer, I. H., Ekaterinaris, J. A., and Platzer, M. F., "A Novel Viscous-Inviscid Interaction Method with Inviscid Wake Modeling," AIAA Paper 94-0178, Jan. 1994.
[5]Ekaterinaris, J. A., Cricelli, A., and Platzer, M. F., "A Zonal Method for Unsteady, Viscous, Compressible Airfoil Flows," *Journal of Fluids and Structures*, Vol. 8, Jan. 1994, pp. 107–123.
[6]McAlister, K. W., Pucci, S. L., McCroskey, W. J., and Carr, L. W., "An Experimental Study of Dynamic Stall on Advanced Airfoil Sections, Pressure and Force Data," Vol. 2, NASA-TM-84245, Sept. 1982.

Numerical Simulation by Cubic-Polynomial Interpolation for Unsteady, Incompressible, Viscous Flow

Hiromi Sugiyama*
Japan Automobile Research Institute, Ibaraki 305, Japan

Introduction

DURING the past three decades there has been significant progress in the numerical analysis of unsteady, incompressible flow problems. Despite the advances in algorithms and computer hardware, however, time-accurate solutions of the incompressible Navier-Stokes (N-S) equations remain a computationally intensive problem, even in two dimensions. Time-accurate solutions of the incompressible flow problems using primitive variables are particularly time consuming because of the elliptical nature of the governing equations. The existing unsteady flow solvers require excessive CPU capability; therefore, there is continuing interest in finding more efficient methods for obtaining numerical solutions to the N-S equations.

Recently, new ideas have been introduced for unsteady flow solvers. One scheme of interest is the cubic-interpolated pseudoparticle-combined unified procedure (CIP-CUP) method, originally proposed by Yabe and Wang[1] and Yabe.[2] The CIP-CUP method is an explicit time-marching scheme with a fractional-step-like approach developed to handle complex fluid flow problems, covering both compressible and incompressible flow. In the CIP-CUP formulation, the solution procedure is divided into two phases: nonadvection and advection. In the nonadvection phase, an intermediate pressure field is solved first, and then intermediate velocity and density fields are obtained from this pressure field. The pressure field is computed by solving a diffusion equation for pressure, which is obtained via manipulation of the momentum and pressure (or energy) equations. In the advection phase, the governing equations are solved for the velocity, density, and pressure at the next time step using the CIP scheme. The CIP scheme is a new class of upwind schemes using cubic polynomial interpolation and is highly accurate for solving generalized hyperbolic equations such as advection-diffusion equations and the Korteweg-de Vries (KdV) equation.[3,4]

In this Note, we present an explicit method, the CIP-artificial compressibility extension (-ACE) method for solving the incompressible N-S equations in a time-accurate and efficient manner. This method uses an artificial compressibility approach[5] to transform the governing equations into a hyperbolic system and uses CIP-CUP methodology to first decouple the pressure and the velocity fields and then to integrate them with respect to time. Although this method is applicable to three-dimensional flow problems, we confine our discussion to one- and two-dimensional flow problems.

Received April 19, 1994; revision received July 19, 1994; accepted for publication July 22, 1994.

*Research Engineer, Research and Survey Division.

Governing Equations

The incompressible N-S equations for isothermal and constant-density fluids are modified by introducing an artificial compressibility approach to the following system of equations, written in tensor notation and dimensionless form:

$$\frac{\partial p}{\partial \tau} = -\beta \frac{\partial u_i}{\partial x_i} \tag{1a}$$

$$\frac{\partial u_i}{\partial t} + u_j \frac{\partial u_i}{\partial x_j} = -\frac{\partial p}{\partial x_i} + \frac{\partial \tau_{ij}}{\partial x_j} \tag{1b}$$

where t is time, $x_i = (x, y)$ are the Cartesian coordinates, $u_i = (u, v)$ are the corresponding velocity components, p is the pressure, τ_{ij} is the viscous stress tensor, and τ and β denote the pseudo-time and artificial compressibility parameter, respectively, which are introduced to apply the artificial compressibility formulation. The viscous stress tensor is defined as

$$\tau_{ij} = \frac{1}{Re}\left(\frac{\partial u_i}{\partial x_j} + \frac{\partial u_j}{\partial x_i}\right)$$

where Re is the Reynolds number. In this formulation, an incompressible flowfield (i.e., a divergence-free flowfield) is only obtained when the pressure field reaches steady state in pseudotime.

Numerical Formulation and Methodology

The CIP-ACE method presented in this Note was developed from the CIP-CUP method.[1,2] As in the CIP-CUP method, Eqs. (1a) and (1b) are divided into a nonadvection phase [Eq. (1a) and $\partial f/\partial t = G$] and an advection phase ($\partial f/\partial t + \boldsymbol{u} \cdot \nabla f = 0$), where f denotes $\boldsymbol{u} = (u, v)$ and G represents the right-hand side of Eq. (1b). The nonadvection and advection phases are then solved separately, as described in the following sections.

Nonadvection Phase

By using a fractional-step-like approach and the Euler implicit time-differencing formula for the time derivative, Eqs. (1a) and (1b) for the nonadvection phase can be written in the following vector form:

$$\frac{\partial p^{**}}{\partial \tau} = -\beta \nabla \cdot \boldsymbol{u}^{**} \tag{2}$$

$$\frac{\boldsymbol{u}^{**} - \boldsymbol{u}^{n}}{\Delta t} = -\nabla p^{**} \tag{3}$$

$$\frac{\boldsymbol{u}^{*} - \boldsymbol{u}^{**}}{\Delta t} = \frac{1}{Re}\nabla^2 \boldsymbol{u}^{n} \tag{4}$$

where the superscript n denotes the quantities at time $t = n\Delta t$, and the asterisk and double asterisks denote the first and second intermediate quantities, respectively. The values with the double asterisks are implicit values introduced by the application of the implicit time differencing.

Here, we briefly describe the essence of the algorithm for solving the system of Eqs. (2–4). First, the velocity and pressure fields are decoupled. Substituting the divergence of Eq. (3) into Eq. (2) gives the following equation:

$$\frac{\partial p^{**}}{\partial \tau} = \beta \Delta t \nabla^2 p^{**} - \beta \nabla \cdot \boldsymbol{u}^{n} \tag{5}$$

Note that this equation is a diffusion equation in pseudotime and can be easily solved by using one of the well-established algorithms (e.g., Golub and Van Loan[6]).

Next, to determine the pressure field that will force the velocity $\boldsymbol{u}^{**}$ to be divergence free, Eq. (5) is solved. When Eq. (5) is iterated in pseudotime until $\partial p^{**}/\partial \tau = 0$, Eqs. (2) and (3) are satisfied, and the divergence of the velocity is zero. Note that at steady state, Eq. (5) is very similar to but is numerically more robust than the market and cell(MAC) method.[7]